

A Multiplex Conversion of a Historical Cinema

Alessio Cascardi (✉ alessio.cascardi@unisalento.it)

Università del Salento <https://orcid.org/0000-0003-2606-0442>

Salvatore Verre

Università della Calabria: Università della Calabria

Alessandra Sportillo

University of Salento: Università del Salento

Gaetano Giorgio

RM Partners

Research Article

Keywords: FEM, beam, reinforced concrete, strengthening, seismic

Posted Date: January 19th, 2022

DOI: <https://doi.org/10.21203/rs.3.rs-945087/v1>

License:   This work is licensed under a Creative Commons Attribution 4.0 International License.

[Read Full License](#)

Version of Record: A version of this preprint was published at Advances in Civil Engineering on March 16th, 2022. See the published version at <https://doi.org/10.1155/2022/2191315>.

A MULTIPLEX CONVERSION OF A HISTORICAL CINEMA

Alessio Cascardi¹, Salvatore Verre², Alessandra Sportillo³ and Gaetano Giorgio⁴*

**Corresponding – alessio.cascardi@itc.cnr.it*

¹ITC-CNR, National Council of Research, Sede Secondaria di Bari – 70124 (Italy)

²University of Calabria, Rende – 87036 (Italy)

³University of Salento, Lecce – 73100 (Italy)

⁴Studio “Giorgio&Partners”, Toritto – 70020 (Italy)

List of Content

13	Abstract
14	Introduction
15	1. Descriptions of the building
16	1.1 Territorial framework
17	1.2 Historical background
18	1.3 In-situ surveys
19	1.3.1 Pacometer
20	1.3.2 SonReb
21	1.3.3 Thermo-camera
22	2. Architectural project
23	3. Seismic upgrading project
24	4. Local beam
25	Geometrical modeling and boundary conditions
26	Materials model
27	Numerical solution
28	Numerical results
29	Conclusions
30	References
31	Acknowledgement
32	Conflict of interest statement

33 **Abstract**

34 The cultural Heritage building is a valuable trace of the past social life for a city. One peculiar typology of
35 building is the theatre or, more recently, the cinema. Within this indoor space, the community of people
36 actively live an emotional feeling over the time causing memories linked to not only the show itself, but also
37 to the place. Furthermore, cinemas are often located in city centers where buildings are historical-oriented form
38 the architectural point of view and for this reason an added-value needs to be recognized. Nowadays, the
39 introduction of pay-TVs has dramatically compromised the cinema business and so-making the turnout of
40 clients more limited. In addition, the recent COVID-19 pandemic situation has further and severally damaged
41 the economy linked to cinema.

42 In this scenario, the modernization and the improvement of old cinemas is becoming an interesting topic in the
43 field of civil engineering. In fact, the new technologies make the experience more comfortable and enthusiastic
44 because of the modern video and audio tools. On the other hand, the expectation of the clients is full-filled
45 when the cinema is able to provide a large choice of views; which means arranging many projection rooms. In
46 order to empathize this aspect, the structural strengthening for a multiplex conversion of an historical cinema
47 is herein reported. The structure required a seismic joint (separating the masonry to the reinforced concrete
48 structural bodies) and a deep strengthening of a very long span beam due to a relevant overloading (in seismic
49 loads combination) caused by the new architectonical project. The numerical simulations demonstrated the
50 validity of different bending strengthening systems (i.e. FRP-plate and *Beton Plaquè*) in terms of both load
51 bearing capacity and maximum deflection. This overview is a part of a larger study in the way of a global
52 structural interventions which will also involve the masonry members.

53

54 **Keywords:** FEM, beam, reinforced concrete, strengthening, seismic.

55 **Introduction**

56 Currently, the construction business is more oriented on the conservation, strengthening and regeneration of
57 existing buildings instead of new constructions. This aspect is particularly felt in the case of the social and
58 cultural building's heritage. In fact, public buildings often cannot be erected in new places since the
59 serviceability and the accessibility are two very linked aspects. Thus, the structures located in city centers need
60 to be focused. An example is the cinema/theatre. In Italy, there are many examples of old cinemas which are
61 now abandoned because not able to cover the modern demand from the public anymore. In fact, the structures
62 are often ancient from the normative point of view (e.g. in seismic capacity) and the projection rooms are
63 inadequate in terms of both the technology and the dimensions/capacity. In order to reuse this important
64 heritage, the seismic update is mandatory while a more functional architectonic project is attended. Therefore,
65 the structural analysis involves many action steps: geometrical and structural survey (diagnostic), global
66 analysis *ante-operam*, choice of the strengthening interventions, design, global analysis *post-operam* and
67 monitoring according to the ISCARSAH's Recommendations, [1].

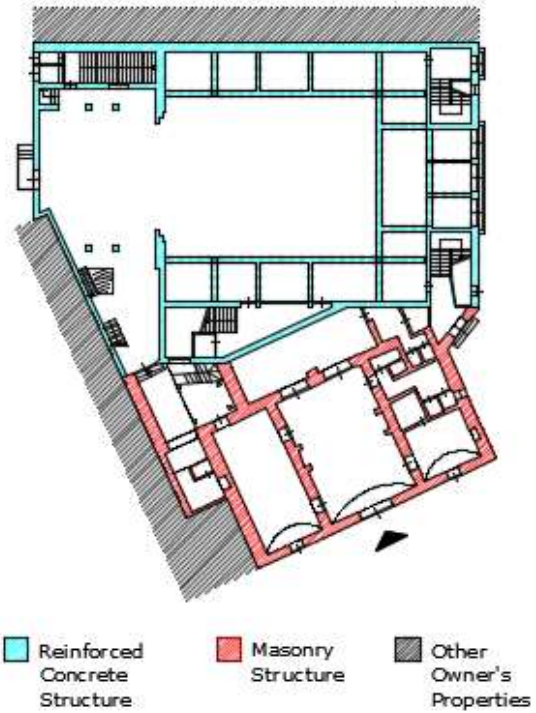
68 In the past decades, there were many examples of cinema reconversions or updating, [2]. For example, in Italy
69 many cinemas were converted into multiplexes in the 2000s following major renovations: the *Cinema Massimo*
70 in Turin, the *Cinema Orfeo* in Milan and the *Cinema Massimo* in Lecce. In particular, the *Cinema Massimo* in
71 Turin was built in the 1930s and had only one auditorium with 1000 seats capacity. It was redesigned a few
72 years later due to the bombings of 1942 (II World War). Following the crisis of the 1980s, the cinema was
73 closed and reopened in 2001 after a renovation. Currently, the *Cinema Massimo* is arranged into three
74 projection rooms: one with 453 seats and two with 147 seats. The *Cinema Orfeo* in Milan was opened in 1936
75 and damaged in 1943 by bombing (again during the II World War). It had a single 2500-seats auditorium and
76 was considered for many years the largest cinema in Milan and among the largest in Europe. In 2004, following
77 a renovation, the cinema was converted into a multiplex with three new rooms: one with 720 seats and two
78 with 290 seats. Finally, the construction of the *Cinema Massimo* in Lecce began in 1939, but it was interrupted
79 during the II World War, only to be resumed later. At the beginning, it had only one theatre with 700 seats.
80 Towards the end of the 1990s, renovation work occurred and the cinema was converted into a multiplex with
81 five auditoriums: one with 675 seats and an opening roof, two auditoriums with 150 seats, one with 144 seats
82 and the last one with 130 seats.

83 In the present paper, the case-study of the ex “*Supercinema*” is reported and discussed. The peculiarities of the
84 selected building are recognizable in its mixed-structure (almost half masonry and half reinforced concrete)
85 and the presence of a very long-span beam which will be the focus of a *Finite Element* (FE) analysis.

86 **1. Descriptions of the building**

87 The so called *Supercinema* is placed in the center of the *Trani*, a quite small city in the south of Italy (see
88 Figure 1a). The structure consists in two adjacent bodies of a different construction system: masonry and
89 reinforced concrete (RC) as illustrated in Figure 1b. An intermediate floor makes the conjunction of the two
90 bodies.

91



a)

b)

92

Figure 1 - The SUPERCINEMA in Trani: a) front view and b) structure typologies individuation.

93

94 Passing throughout the main entrance, according to the original functional conception (Figure 2a), the building
 95 has a load-bearing masonry structure, consisting of two elevations above the ground. At the ground floor, the
 96 one used for the cinema/theatre purpose, an entrance hall is dominating the space; while a small projection
 97 room (Figure 2b) is on the left opposite to the offices and toilets. The roofs of the first level are barrel vaults,
 98 with a maximum height of 5.20 m. Before entering the theatre, a short-lived of the transition area under the
 99 conjunction floor is found. It is a single-story area consisting of a connecting slab. Here, a corner bar is placed
 100 (Figure 2c and d). The reinforced concrete building which houses the theatre consists of three floors above
 101 ground and one basement, all of them can be accessed by stairs located at the corners. On the ground floor
 102 there is the stage and the stalls, currently without seats, while on the first and second floors there are two
 103 galleries that will be converted into recreational areas (on the first floor) and three additional halls (on the
 104 second floor) as better shown in the next sections. When entering within the core of the theatre, a very long
 105 span beam, supported on octagonal cross-section columns, dominate the structural behavior and the
 106 architectural view (Figure 2e). The mentioned span is about 14 m and therefore much longer than the others,
 107 which on average have a length of 4.00 m. For this reason, a series of transversal beams were constructed in
 108 order to limit the potential mid-span deflection (Figure 2f and g). The other beams are supported by prismatic
 109 cross-section columns (Figure 2h). The whole photos views are reported in Figure 2I in order to make the
 110 understanding of the building conceptual design cleaner and easier.

111 There were about two thousand seats, which are currently dismantled. The floor height of the stalls ranging
112 between 6.00 m to 9.90 m, while the height of the galleries on the second and third floors is about 2.75 m.
113 Instead, the height of the stage is 12.00 m.



a)



b)



c)



d)



e)



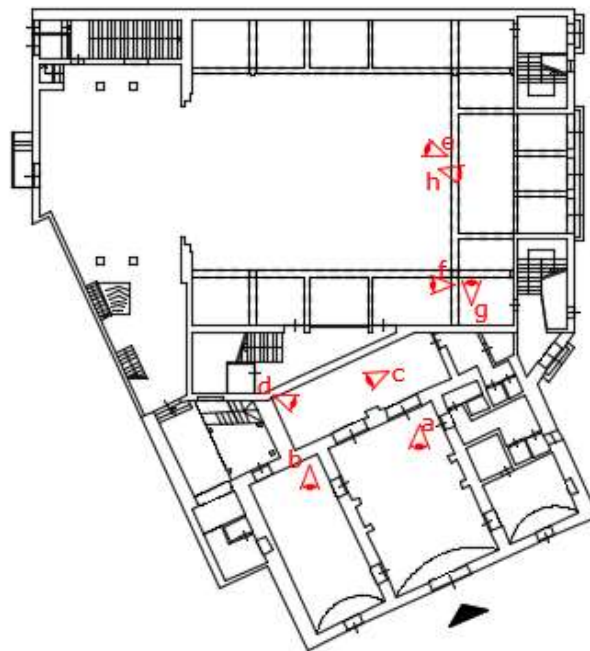
f)



g)



h)



i)

Figure 2: a-h) inside photos and i) plan with trigger points

114

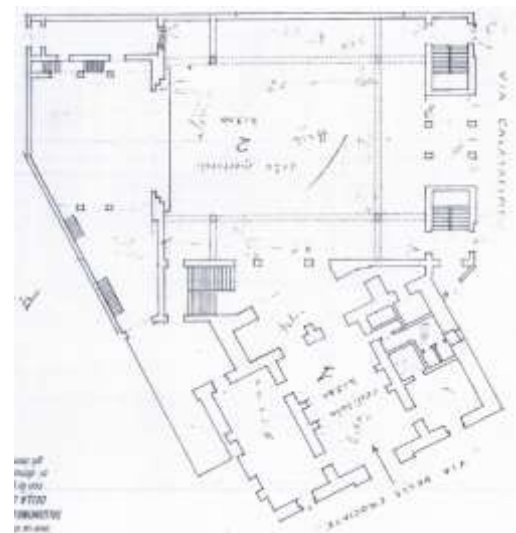
115 1.1 Territorial framework

116 *Trani* is located on the Adriatic coast, 45 km north from Bari. Together with *Andria* and *Barletta*, it makes one
 117 of the six provincial capitals of the *Apulia* region. According to an ancient legend, the name *Trani* is linked to
 118 *Tyrrhenus*, son of the Greek mythological hero Diomedes, who founded the city in the 3rd century a.C.
 119 However, some modern scholars have established two different hypotheses regarding the origin of the name:
 120 the first is that *Trani* may be the shortened form of *Trajan* (a name that may have been given to the city in
 121 honor of the Roman Empire) and the second is that the name derives from the medieval term “*trana*”, which
 122 indicated an inlet suitable for fishing: an inlet that currently corresponds to the city port. In urban terms, *Trani*
 123 is divided into three main areas:

- 124 • the historic center, surrounded by huge masonry walls by 1846, embellished by palaces and historical
125 monuments, as well as, by narrow and winding streets. It is the most characteristic area of the city,
126 close to the port and the cathedral.
- 127 • Nineteenth-century village, a wealthy and aristocratic area, characterized by villas and palaces of the
128 period. The Supercinema falls within this area.
- 129 • A residential and modern area, which grew rapidly at the beginning of the 20th century due to the
130 expansion of the city. It branches off beyond the 19th-century village, mainly to the south towards
131 *Bisceglie* and from the 1950s also to the west towards *Andria* and *Corato*. There were no expansion
132 northwards towards *Barletta* due to the presence of the industrial area.

133 1.2 Historical background

134 The Supercinema was commissioned by Giuseppe Boccasini, who had returned to *Trani* after making his
135 fortune in America, Domenico Di Mango, foreman of the Aswan dam and an expert in reinforced concrete
136 structure, Domenico Persano, a large landowner from Lecce, and Nicola Guacci, stationmaster, with his wife
137 Lucia Laurora. The Figure 3 (left) shows the principals of the Supercinema at the early-stage construction. The
138 on-site activities began in 1934 under the supervision of the engineer Enrico Bovio and the inauguration took
139 place the following year, arousing great amazement from the Trani public and numerous foreigners who
140 flocked to the town to see a film in the area's first state-of-the-art cinema, even though it was the only cinema
141 with about two thousand seats (see Figure 3 right).



142
143 *Figure 3: Historical photos: principals (left) and original structure design (right).*

144 The theatre has undergone several modifications:

- 145 • in 1991 the renovation of the installations, the stage and the dressing rooms;
- 146 • in 1991 the construction of a false ceiling;
- 147 • in 1995 the general renovations and adaptations;

148 • in 2002 the construction of a new hall to replace the second gallery and the conversion of an internal
149 room into a projection room.

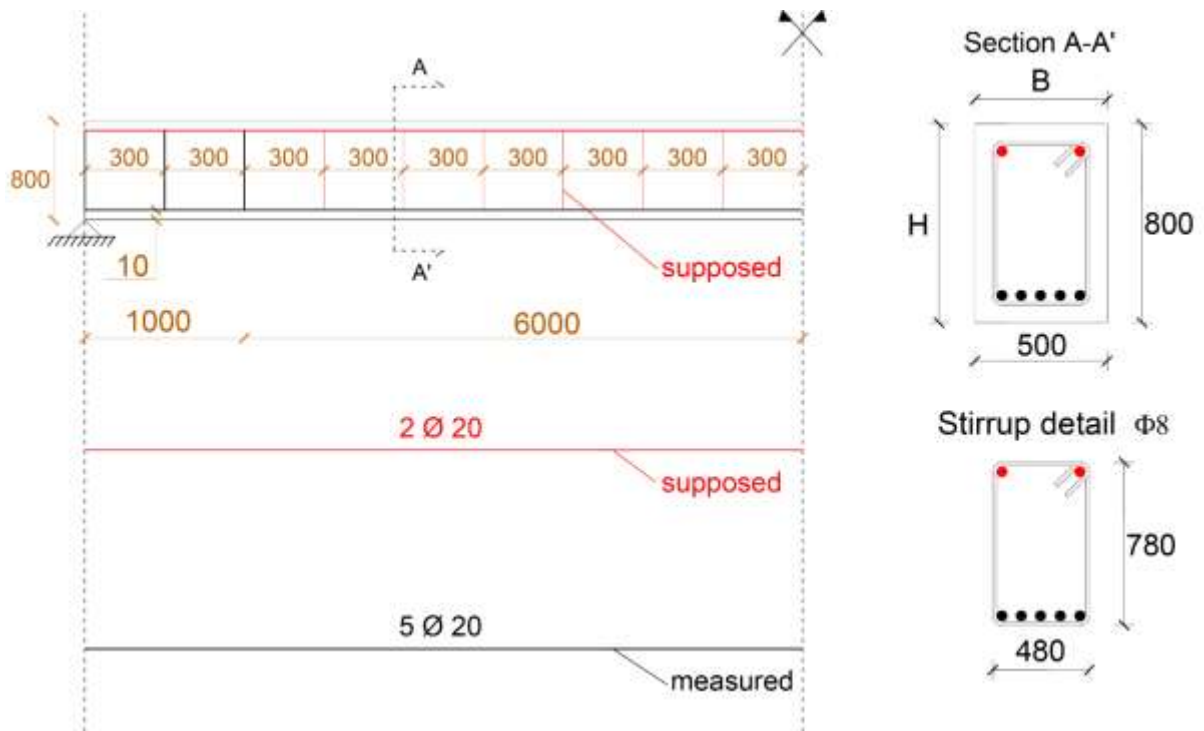
150 However, it has now been closed since 2008 and subjected to historical and architectural restrictions. In April
151 2019, the removing of the asbestos roof was performed.

152 **1.3 In-situ surveys**

153 The accuracy of a structural strengthening design is based, above all, on the initial knowledge mining phase,
154 by carrying out a preliminary test campaign that investigates the mechanical properties of the construction
155 materials, the geometry, the state of decay, the level of damage, etc. According to Italian code NTC 2018 [3]-
156 [4], based on the quantity and the typology (destructive or not destructive) of the investigations carried out in
157 the cognitive phases, a certain LC (*Level of Confidence*) is reached. The LC has three options: LC1, LC2 and
158 LC3. As a congruence, a corresponding partial factor is identified, namely the CF (*Confidence Factors*), which
159 can assume the value of 1.35, 1.2 and 1 respectively. The aspects that define the levels of confidence are:
160 geometry of the structure, construction details, material properties, connections between the various elements
161 and their presumed modes of collapse. The confidence factor is used for the reduction of the average values of
162 the mechanical parameters from in-situ tests (e.g. strength of the materials) and must be understood as
163 indicators of the level of detailing achieved. Concerning the herein reported case-study, only the RC building
164 was investigated by performing non-destructive tests. Instruments used were the pacometer, the thermo-camera
165 and the combined *SonReb* test. Therefore, the investigations were limited at that moment providing a LC1 and
166 a FC=1.35. More details of the diagnosis are reported in the following sections.

167 **1.3.1 Pacometer**

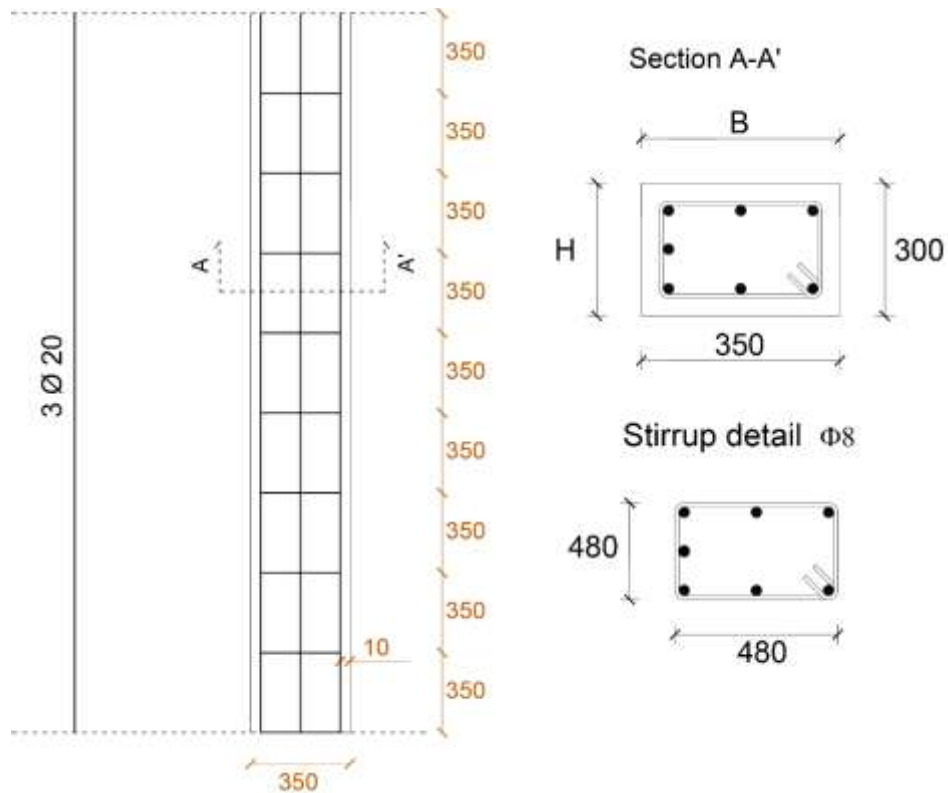
168 In the Supercinema, the pacometric tests were carried out on the beam with a 13.9 m span and on the 30x35
169 cm rectangular cross-section columns near the exits on the opposite side of the platform. By referring to the
170 beam (see Figure 4), the recordings revealed that the cross-section has uniform concrete cover with 1-2 cm
171 thickness, a total of 5 ϕ 20 bottom longitudinal reinforcement rebars and ϕ 8/30cm stirrups, although the span
172 was not constant. The upper longitudinal reinforcement was assumed equal to 2 ϕ 20 to be on the conservative
173 side. On the other hand, the column (see Figure 5) figured out an almost uniform concrete cover with 1-2 cm
174 thickness, a set of 3 ϕ 20 longitudinal rebars per side and ϕ 8/35 cm arranged for transversal reinforcement.



175

176 *Figure 4 - Identification of internal reinforcing bars of the very long span beam: cross-section (left) and longitudinal section (right).*

177



178

179 *Figure 5 - Identification of internal reinforcing bars of the column: cross-section (left) and longitudinal section (right).*

180

181

1.3.2 SonReb

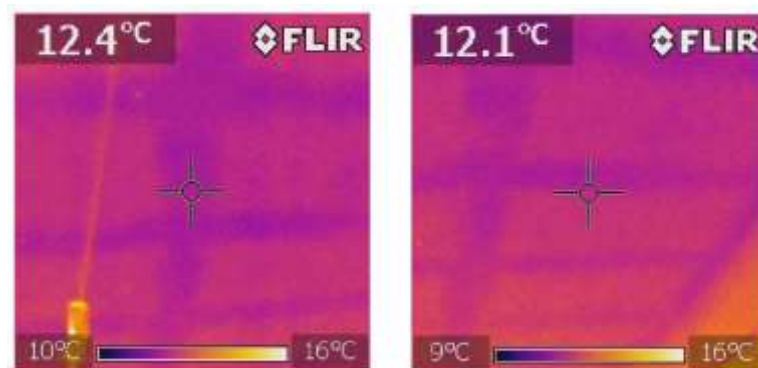
182 The in-situ compressive strength of concrete can be influenced by numerous factors, such as carbonation,
183 amount of internal reinforcing steel, as well as, their location and/or the aggregate size. It is well-known that
184 the most accurate compressive strength estimation can be determined by combining different testing
185 techniques. For example, the correlation of data from the *Schmidt hammer* and *ultrasonic tester* to the existing
186 compressive strength data is one of the more accurate predictor investigations. Researchers have developed an
187 algorithm whereby the rebound value from the Schmidt hammer and the compression wave velocity from the
188 ultrasonic test can be correlated with actual compressive strength of the concrete. The correlation of the
189 different testing methods with actual compressive strength is commonly known as the SONREB (i.e. *SONic*
190 *REBound*) method. The conducted investigation in the *Supercinema* were performed on a series of two beams
191 and four columns and provided an average compressive strength of the concrete equal to ~23 MPa. The
192 measures had a scatter <10%, thus no more investigations were needed since the quality of the concrete can
193 be considered uniform in the RC structure.

194

1.3.3 Thermo-camera

195 The area in front of the bar (see again Figure 2c and d) was roofed with a horizontal floor covered by a plastic-
196 based countertop. The latter, when partially removed, allowed to point out the thermo-camera. The result is
197 shown in Figure 6. A floor connecting the masonry and RC structures emerged by the difference in
198 temperature. It is evident the scheme of the joists (at 9-10°C) and the brick pots (at 14-16°C). this floor was
199 joined to the structures by a simply supported lateral beams (Figure 7). Furthermore, using a laser meter, it
200 was discovered that the soffit of the floor is at an intermediate height between the soffit of the masonry building
201 and the soffit of the reinforced concrete building according to Figure 8.

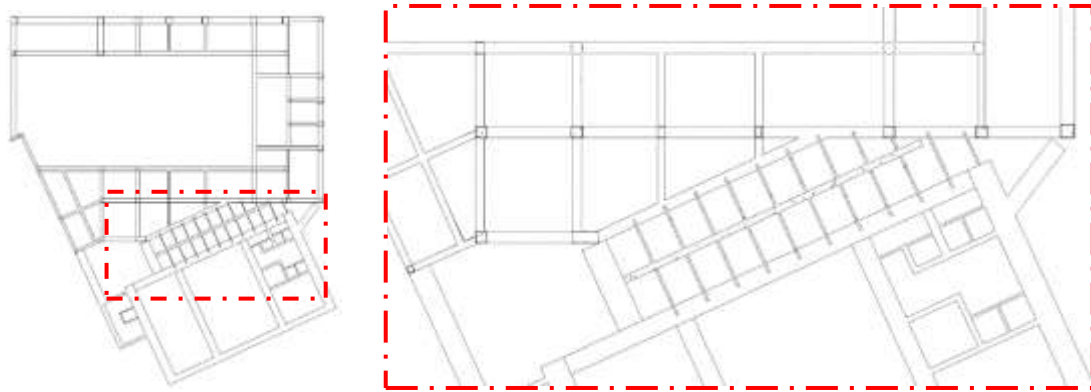
202



203

Figure 6 - Thermo camera outcomes.

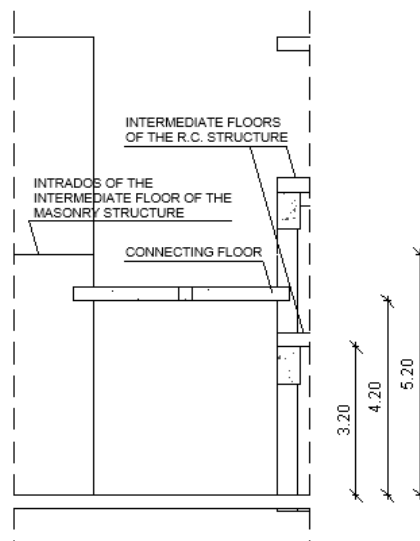
204



205

206

Figure 7: Detail of the connecting floor: identification (left) and zoom (right).



207

208

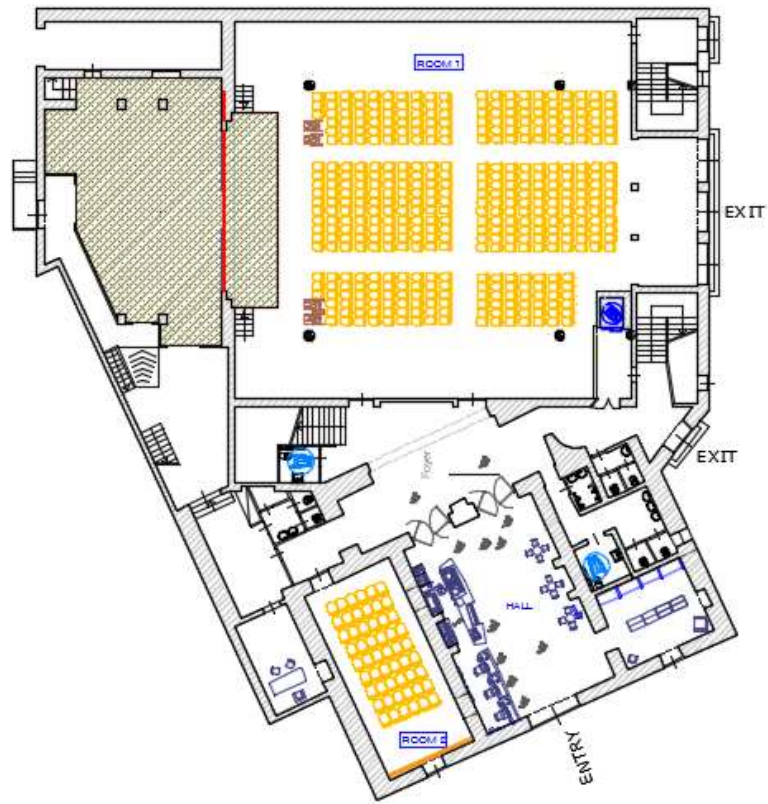
209

Figure 8: Transversal view of the connecting floor.

210 2. Architectural project

211 The *Supercinema* is intended to be converted from a cinema-theatre to a multiplex with five projection rooms
212 (three new) and different areas for entertainment and/or alternative use. While, the layout and functionality of
213 the individual rooms within the masonry building are planned to be maintained unaltered according to Figure
214 9. So, an entrance with a box office and bar corner, the auditorium (ROOM 2), the office and a bookshop
215 corner are prepared. On the ground floor of the reinforced concrete building, the stalls in ROOM 1 will be
216 renovated. On the first floor (see Figure 10), the galleries to the side of the stage will be converted into an
217 alternative use of the space with tables and chairs, while the one in front of the stage will remain in its original
218 function. On the second floor, the galleries at the side of the stage will become two halls (ROOM 3 and ROOM
219 4) following the 1.80 m extension of the ceiling, while the one at the front will become an additional hall
220 (ROOM 5) as shown in the Figure 11. Furthermore, toilets for the disabled and lift shafts will be added. The
221 architectural design envisages seating arrangements as follows: 54 seats for ROOM 2, 416 seats for ROOM1,

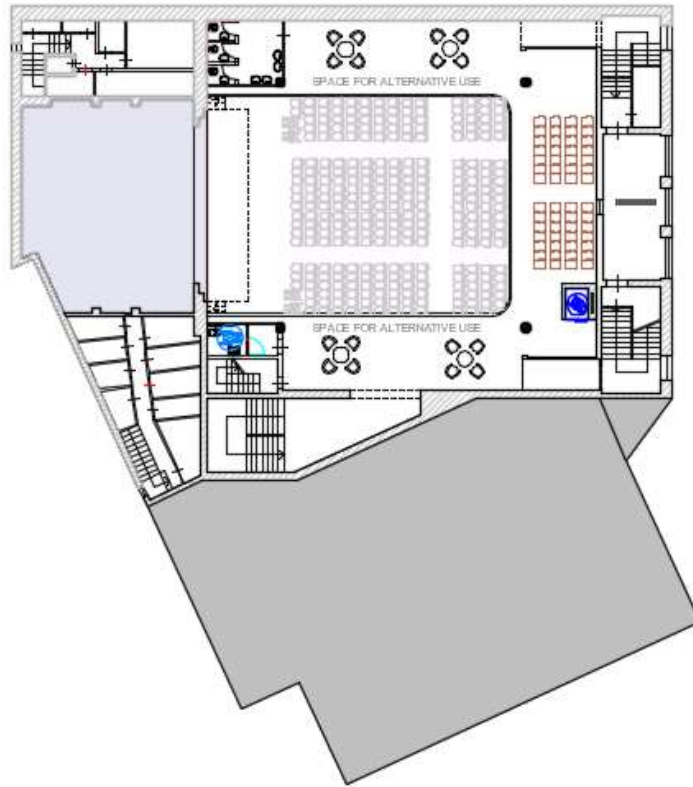
222 56 seats for the first-floor gallery, 58 for ROOMS 3 and 5 and 63 for ROOM 4, for a total of 705 seats. A few
223 render views are illustrated in Figure 12 in order to give an idea of the project when completed.



224

225

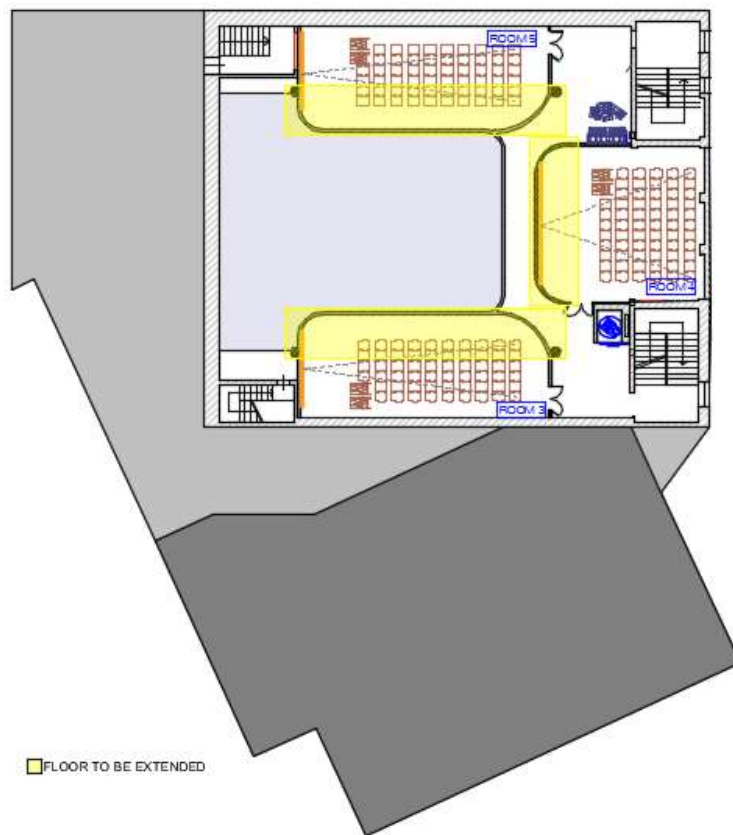
Figure 9: Ground floor layout.



226

227

Figure 10: First floor layout.



228

229

230

Figure 11: Second floor layout.



a)



b)



c)



d)

Figure 12 - Render simulation of the Supercinema: a) recreation area, b) ROOM2 and c-d) ROOM1.

231

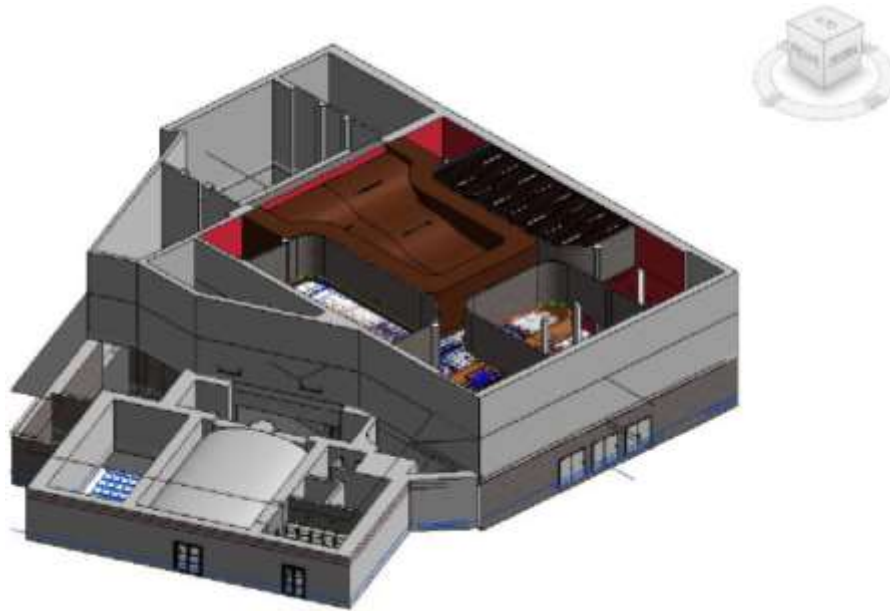
232 Expanding the floor between the second and third decks in order to create three new halls at the current galleries
 233 means a higher load due to both crowding and the presence of seats that will act at along the almost 14 m long
 234 span of the beam which is already poorly reinforced. Therefore, in the following paragraphs, the bending
 235 behavior of the beam will be studied, constrained at the ends by two simply supports in order to maximize the
 236 deflection in the middle-span cross-section. Moreover, the strengthening is also simulated. In particular, the
 237 beam was studied using finite element software, i.e. MIDAS FEA NX [5], and the bending reinforced was
 238 proposed because of the Superintendence advised against the construction of a new support column at the
 239 middle span of the overloaded beam. In this scenario, the use of composite materials, i.e. carbon fiber plate
 240 (CFRP) installed on the intrados, is a suitable solution by taking advantage of their lightness, high mechanical
 241 strength and high resistance to corrosion. In addition, reinforcement was also studied using metal
 242 reinforcement plate on the intrados and extrados of the beam, connected by connectors.

243 3. Seismic upgrading project

244 Transforming the cinema into a multiplex, changing the serviceability load of the building, does not only mean
 245 architecturally designing the arrangement of the rooms, but also possibly increasing the demand of a structural
 246 element; therefore, the bending behavior of the beam on which the floor to be extended was studied and its
 247 structural reinforcement was designed. With the help of Autodesk Revit software [6], which uses the BIM

248 (Building Information Modeling) methodology, starting from the architectural model (Figure 13a), the
249 structural model (Figure 13b) was built with the structural elements (beams and columns with their
250 reinforcements and load-bearing walls).

251



252

253

a)



254

255

b)

256

Figure 13 - Supercinema: a) architecture and b) structure evidences.

257 Since the masonry building has not been investigated and since the two structures are made of different
258 construction materials, a seismic joint was designed for separating the two bodies and avoids the phenomenon

259 of hammering in the event of an earthquake. Particular attention must be focused when two buildings are
 260 placed next to each other, since in the event of seismic action they will have a different response in terms of
 261 lateral displacement depending on their mass and stiffness despite being subjected to the same ground
 262 acceleration since having a different and independent vibrating mode. Therefore, the joint must ensure an
 263 adequate reciprocal distance between two adjacent buildings, whether new or existing. This distance was
 264 foreseen in the design phase by calculating the displacements, due to seismic action, of the points of the
 265 constructions facing each other and respecting the minimum limits foreseen by the technical regulations.
 266 According to the NTC 2018, a distance between two adjacent constructions must be ensured such as to avoid
 267 hammering, which is equal to:

$$268 \quad \frac{1}{100} \cdot \frac{2 \cdot a_g \cdot S}{g} \cdot h$$

269 With:

- 270 • h building height;
- 271 • a_g maximum horizontal acceleration at the site;
- 272 • g acceleration of gravity;
- 273 • S coefficient considering the subsoil category and topographical conditions, equal to: $S = S_S \cdot S_T$;
- 274 • S_S stratigraphic amplification coefficient;
- 275 • S_T topographic amplification coefficient.

276 To calculate the maximum horizontal acceleration at the site, the parameters related to the site were considered
 277 as following listed down:

- 278 • nominal life (50 years);
- 279 • class of use (III);
- 280 • reference life (75 years);
- 281 • spectrum (SLV 10%);
- 282 • probability of exceeding the reference life (10%);
- 283 • return period (712 years).

284 The outcomes are reported in Table 1.

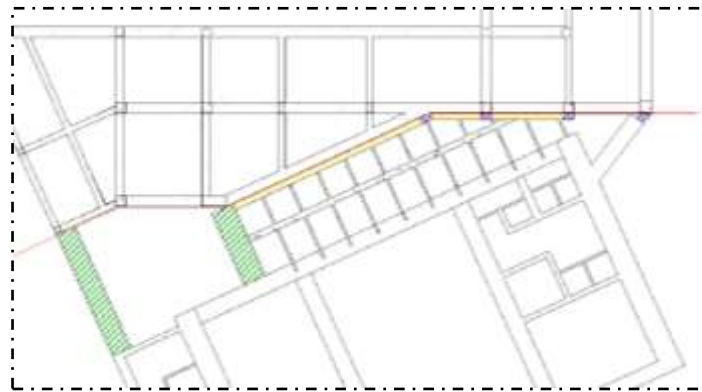
285 *Table 1 - Seismic data.*

h	S_S	S_T	a_g/g	F₀	T_c
[m]	[-]	[-]	[-]	[-]	[s]
9.90	1.20	1.00	0.107	2.5	0.37

286

287 A minimum distance between the two buildings of 4 cm was computed. As can be seen in the Figure 14, in
 288 order to separate the two buildings (red line), the load-bearing walls need to be cut (indicated by the green

289 hatching), a 30 cm beam is created (indicated by the yellow hatching) on which the connecting floor will rest,
290 and 3 rectangular 50x30 cm pillars and 1 trapezoidal pillar are built (indicated by the blue hatching).



291

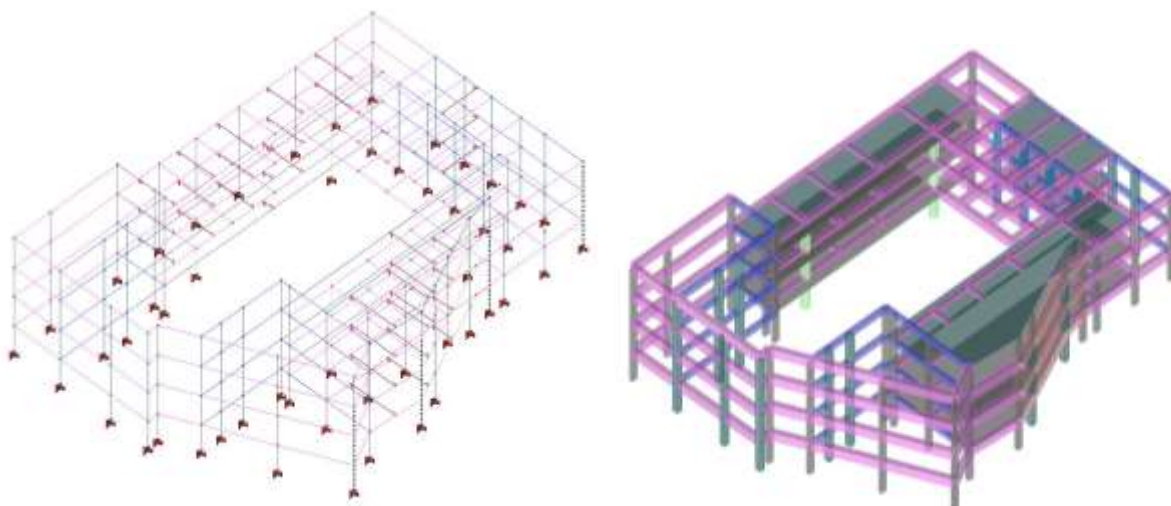
292

Figure 14 - Seismic joint location.

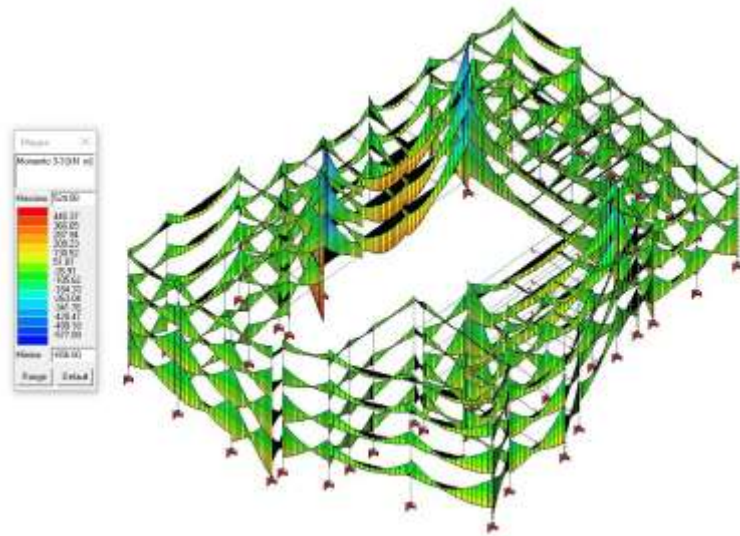
293 The use of BIM was useful in the transition from the architectural model to the structural model in order to
294 better understand the *skeleton* of the two structures and to be able to produce the joint in a feasible way. The
295 global behavior of the structure was studied using the PRO_SAP [7] finite element calculation software in
296 order to evaluate and verify the principal stresses. Only the reinforced concrete building was modelled by
297 inserting beams, columns and floor frames. The constrains were perfect fixed type. The model and the acting
298 stresses represented in the Figure 15a and b were obtained. It is evident as the critical element is the very long
299 span beam, which figured out the maximum bending stress (see redo color in Figure 15b). In particular, the
300 value of the load acting on the beam, with the most unfavorable combination (seismic combination), is 52.89
301 kN/m: this value was then inserted as a uniformly distributed load on the beam span to carry out the analyses
302 with the Midas FEA NX software.

303

304



a)



b)

305

306

307 *Figure 15 - RC-structure global model in seismic load combination without any strengthening: a) beam and 3D model and b) results.*

308 **4. Local beam**

309 The bending deficiency of the *very long span beam* (VLSB), about 14 m, was before mentioned. The problem
 310 is related to two main aspects: the high sustained load on the span itself ratio and the poor-quality concrete
 311 with the modest internal steel strengthening (both stirrups and longitudinal steel rebars). Therefore, the bending
 312 strengthening was focused on the *External Bonded* (EB) systems and designed by means of *Finite Element*
 313 *Method* (FEM). In particular the use of laminate plates was considered by comparing two different materials:
 314 carbon (CFRP - *Carbon Fiber Reinforced Polymer*) and steel (BP - *Beton Plaquè*). The numerical procedure
 315 was assessed using the commercial code MIDAS FEA NX [5]. It is in the knowledge of the authors that the
 316 majority of the RC beams tested in the laboratory have a length ranging in 3-5 m according to the literature,
 317 [8]-[11]. In particular, the adopted test setup is simply supported with punctual applied load (P) in almost all
 318 cases. In [12] it is possible to observe the continuous (on three supports) RC beams with an exceptional length
 319 of 8.5 meters, but the test setup adopted reported the RC beams with two bending spans of 4.25 m. In [13] it
 320 is possible to observe different boundary conditions, at one end the RC beams was clumped while at the other
 321 end a torsional constraint in order to test beams at torsion. Finally, the literature regarding the case study
 322 presented in this work (type applied load and the entire RC beam long) is poor.

323 **Geometrical modeling and boundary conditions**

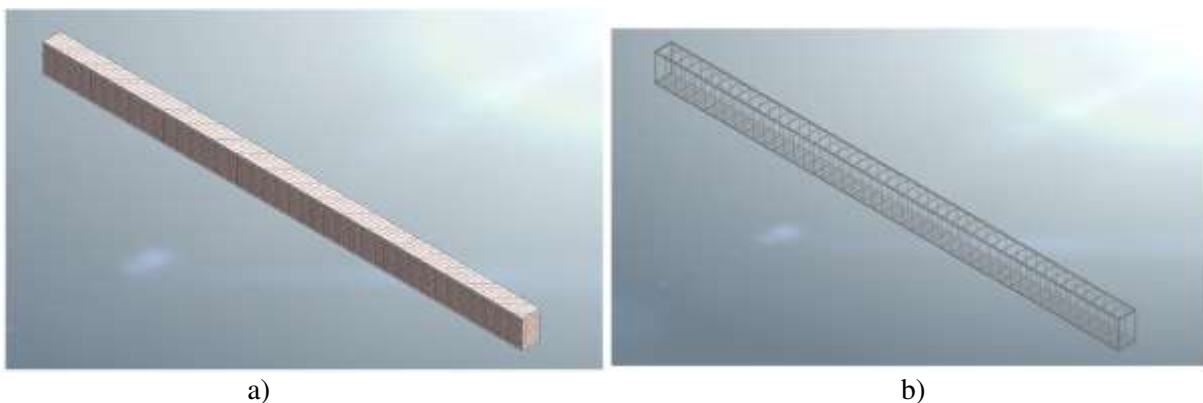
324 The beam was three-dimensions (3D) modelled in order to replicate the entire beam in the most reliable way.
 325 Since the imposed load was full-gravitational oriented, the end constrains were simulated to be reactive only
 326 against the vertical translation. In addition, one of the ends constrains was also set to avoid the horizontal
 327 translation in the perspective of numerically consider an isostatic structural member. However the considered
 328 beam is a continuous element simply supported by many columns (more than two), the static schema was
 329 assumed to be the uniformly distributed load on double supports. It is felt by the authors that the choice is

330 consistent with the real case study since the critical span was highly longer than the others while the
 331 overloading is acting only on it. Moreover, the limited number of the internal rebars, associated to their level
 332 of corrosion, are both factors indicating that a rotation at the ends of the VLSB is potentially reliable and,
 333 anyway, on the conservative side. The geometry and the internal reinforcement are both illustrated in Figure
 334 4. This modelling technique, find in literature [14]-[21], is useful for establishing the real behavior and the
 335 complete crack pattern along the entire beam. The beam was modelled using a structured mesh with tetrahedral
 336 type elements. The characteristic element length equal to 10mm was evaluated through the relationship
 337 provided by Midas:

$$338 \quad h = \sqrt[3]{(\text{volume of mesh})}$$

339 The internal reinforcement was modelled through a linear truss, while the external reinforcement was modelled
 340 by a shell element with linear interpolation functions. Finally, a perfect bond was assumed between the beam
 341 and external reinforcement and the concrete and internal reinforcement. In Figure 16, a 3D FE mesh was
 342 reported. In particular, the adhesion between the concrete and the reinforcing rebars was defined through the
 343 internal function called embedded regions. The embedded technique is used to specify that the internal
 344 reinforcement is embedded in host elements (beam).

345



346
 347
 348
 349

Figure 16 - Geometrical modelling and FE resolution: a) concrete and b) internal reinforcement.

350 **Materials model**

351 The concrete smeared cracking function was used to model the two principal concrete failure mechanisms such
 352 as the tensile cracking and the compressive crushing. This model is designed for applications in which the
 353 concrete is subjected to essentially monotonic loading and it uses oriented damaged elasticity concepts
 354 (smeared cracking) to describe the reversible part of the material's response after cracking failure. The
 355 constitutive compressive law of concrete was modelled by non-linear relationship proposed by *Thoronfeldt et*
 356 *al.* [22].

357

$$\frac{f}{f_c} = \frac{n \left(\frac{\varepsilon}{\varepsilon_c} \right)}{(n - 1) + \left(\frac{\varepsilon}{\varepsilon_c} \right)^{nk}}$$

358 where f_c and ε_c are the compressive strength and relative strain, while the parameter n is possible to define it
 359 by the equation:

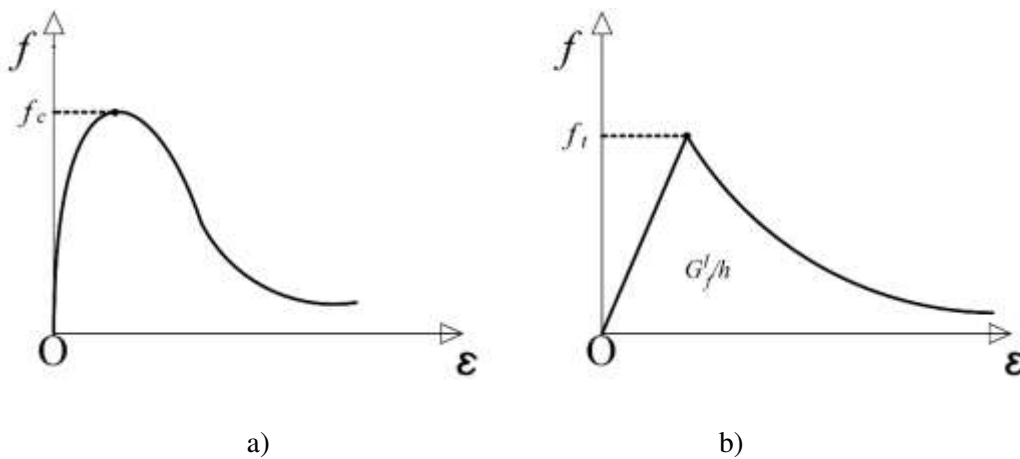
360
$$n = 0.4 \cdot 10^{-3} f_c + 1$$

361 The descending branch of the stress-strain relation multiplying the power n by a coefficient k , it is possible to
 362 define it by means of the equation

363
$$k = 1 \quad \text{for} \quad 0 > \varepsilon > \varepsilon_c$$

 364
$$k = 0.67 + \frac{f_c}{62} \quad \text{for} \quad \varepsilon \leq \varepsilon_c$$

365 The constitutive tensile law was modelled by the relationship proposed by *Hordijk*, [23]. The model's
 366 parameters used are the tensile strength $f_t=1.59$ MPa, the fracture energy $G_f=0.08$ N/mm and the crack band
 367 $h=62$ mm. In Figure 17 the materials constitutive laws were reported.



370 *Figure 17 - Material constitutive laws: a) compression and b) tension.*

371 The steel constitutive law used to model the longitudinal steel and the stirrups was considered by means of
 372 elastic-plastic hardening trend, both in tension and compression. In the linear elastic range, the behavior has
 373 been defined by the density ($\rho = 7.85$ g/cm³), *Young's modulus* ($E_s = 210$ GPa) and *Poisson's ratio* ($\nu = 0.3$).
 374 Instead, the plastic-hardening branch has been defined through the yield strength (equal to 356 MPa), the
 375 ultimate strength (equal to 856 MPa) and the deformation values corresponding to the two strengths
 376 considered.

377 The investigated beam was reinforced with two reinforcement systems CFRP and BP. Both systems were
 378 modelled as a homogenous material by a shell element with the linear interpolation functions. Therefore, the
 379 constitutive tensile laws were linear elastic until failure for the CFRP system, while linear elastic until the yield
 380 stress and then perfect plastic for BP-system. The input data parameters are modulus (E_t), thickness (t), yield
 381 stress (f_y) and the ultimate strain (ε_u) and they were summarized in Table 2. In addition, the CFRP system has
 382 been applied on a part of the beam width equal to 15 cm in the tension zone, while the BP system was applied

383 on the whole beam width. In particular, the external reinforcement was applied both in the flexural compression
 384 and tensile side of the existing beam. The two steel plates, in the numerical model was not connected.

385 *Table 2 - Parameters for the EBs.*

External Reinforcement	E [GPa]	t [mm]	f_y [MPa]	ϵ_u [%]
CFRP plate	170	1.4	-	1
BP	210	5	275	2

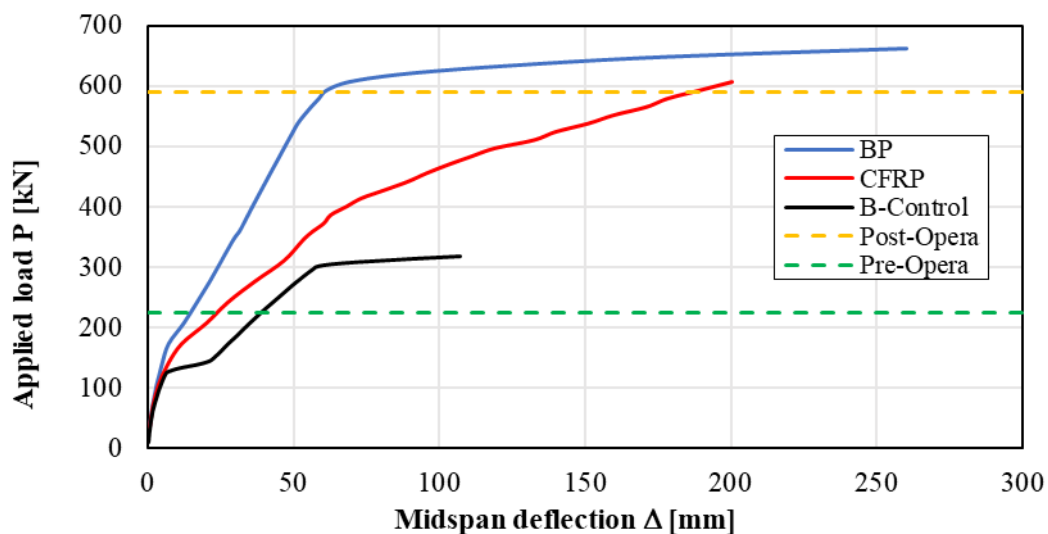
386

387 Numerical solution

388 The analysis was conducted under enforcing displacements $-\lambda u$ in y -directions and the nonlinear equations
 389 were solved by the well-known *Newton's modified method*. The aim is to recompute the global stiffness of
 390 the structure at each load step. Consequently, the method is costly from the computational point of view in the
 391 n -step while faster at global level. Moreover, Newton's modified method for determining a root of a nonlinear
 392 equation $f(x)=0$ has long been favored for its simplicity and fast rate of convergence. *Newton's modified*
 393 *method* iteratively produces a sequence of approximation that converge quadratically to a simple root. While
 394 a few rules with higher order convergence have long been known, these have the disadvantage of requiring
 395 higher order derivatives.

396 Numerical results

397 The Figure 18 shows the numerical curves in terms of applied total load versus mid-span section deflection.
 398 In addition, the dashed lines indicate the load value to which the existing beam is currently subjected, which
 399 is equal to 224 kN (green line), and the load to which it will be subjected after the change of serviceability of
 400 the building and, at the same time, the extension of the floor (see Section Architectural project) or rather equal
 401 to 589 kN (orange line).

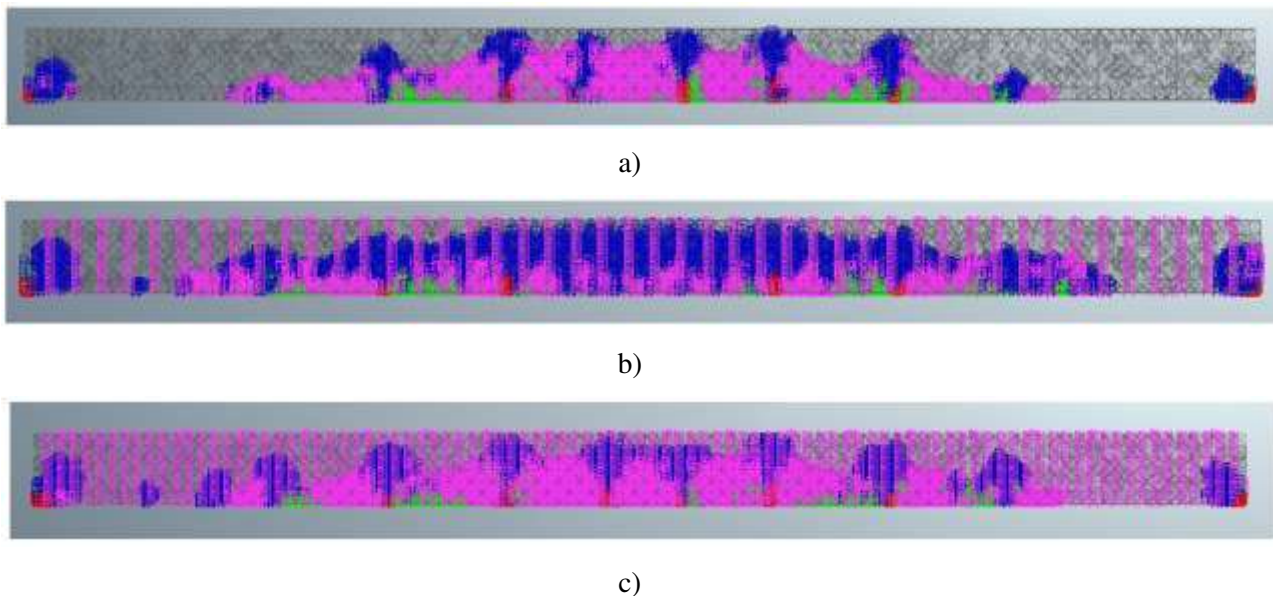


402

403

Figure 18 - Load vs deflection law: comparison of the results.

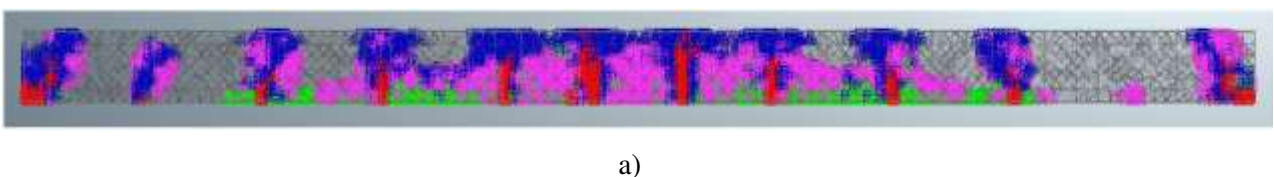
404 First of all, from the Figure 18 it can be seen that the actual capacity of the beam (black line) is largely major
405 of the potential original design load (i.e. 224 kN), while it is dramatically minor when compared with the
406 demand reached after the multiplex conversion (i.e. 589 kN). The red and blue numerical curves represent the
407 reinforcement scenario of the existing beam with CFRP and BP, respectively. Both the reinforcement systems
408 resulted, in terms of applied load, to have greater load bearing capacity if in contrast with the required limit
409 load, again 589 kN. On the other hand, the bending capacity expressed in terms of deflection is a further crucial
410 aspect. In fact, the CFRP solution exhibited a larger deformation (i.e. 200 mm) at the mid-span level when
411 compared with the BP alternative before the yielding (i.e. 61.44 mm). nonetheless, in both cases the deflection
412 is relatively low if normalized per the span of the beam providing an optimal solution in order to take into
413 consideration of the limitations in the Italian standard [3]. Furthermore, the stiffness in the elastic range is
414 considerably higher for BP instead of CFRP. The reliability of the proposed FE model is testified also by the
415 evaluation of the failure modes. At this scope the comparison of the crack patterns at the first crack opening
416 step and at the ultimate limit state condition are illustrated in Figure 19 and Figure 20, respectively. As
417 expected, the first crack (in red) opens at mid-span level and the next one trend to have constant distance each
418 other in between two consecutive stirrups. By observing the ultimate state, the development of the cracks
419 (again in red) is more evident with a pseudo vertical trend. It is also noticeable that the number of cracks is
420 almost the same in all the configurations.

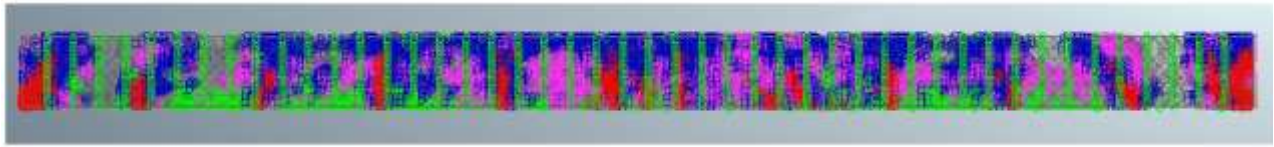


421 *Figure 19 - Crack pattern when the first crack opening: a) B-Control, b) CFRP and c) BP.*

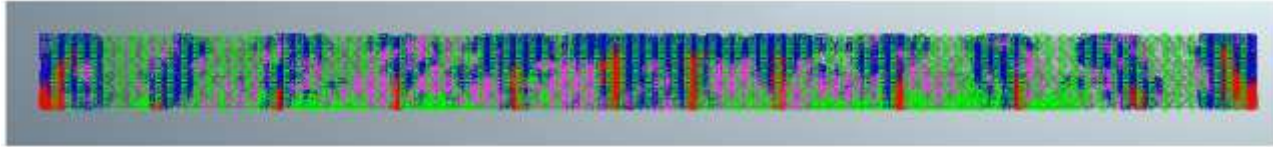
421

422





b)



c)

Figure 20 - Crack pattern at ultimate limit state: a) B-Control, b) CFRP and c) BP.

423

424 **Conclusions**

425 The case study herein presented report on the common problem of overloading and seismic deficiency due to
 426 the chance of serviceability of a cultural heritage: the *Supercinema* in *Trani* (Italy). The study dealt with a
 427 scientific key, or rather the aid of advanced tools for surveying, analyzing and verifying the structures. In order
 428 to be able to carry out the three new projecting rooms in correspondence with the current galleries on the
 429 second floor, it was decided to design the attic between the second and third deck. In these new rooms, the
 430 overloading was fully located on an approximately 14 m long span RC beam.

431 Before proceeding with the study and reinforcement of the beam, since the building is composed of two
 432 adjacent structures of different construction system, the structural model was first developed, starting from the
 433 architectural model, thanks to the help of the Autodesk Revit BIM software that allowed to better understand
 434 the position of the structural elements. Subsequently, a seismic structural joint was designed in order to
 435 "separate" the two structures.

436 Secondly, modeling the beam within the Midas FEA NX finite element software was performed aiming to
 437 simulate the bending strengthening by means of both CFRP-plate (CFRP) and *Beton Plaquè* (BP), in a non-
 438 linear static analysis. The results demonstrated the effectiveness of the two proposed solutions in terms of both
 439 load bearing capacity and mid-span deflection.

440 **References**

- 441 [1] ICOMOS/Iscarsah Committee. (2005) Recommendations for the analysis, conservation and structural
 442 restoration of architectural heritage. See www.icomos.org
- 443 [2] Berlucchi, N., & Cicognetti, S. (2020). Restauro e adeguamento normativo di un teatro all'italiana: il
 444 Sociale di Camogli. Restauro e adeguamento normativo di un teatro all'italiana: il Sociale di Camogli,
 445 27-42.
- 446 [3] NTC 2018 – Nuove norme sismiche per il calcolo strutturale. Decreto Ministeriale 17 gennaio 2018.
 447 [in Italian].

- 448 [4] CIRCOLARE 21 gennaio 2019, n. 7 C.S.LL.PP. Istruzioni per l'applicazione dell'«Aggiornamento
449 delle “Norme tecniche per le costruzioni”» di cui al decreto ministeriale 17 gennaio 2018. [in Italian].
450 [5] F.E.A. Midas, ‘Advanced Nonlinear and Detail Program, Analysis and Algorithm (1989).
451 [6] Khemlani, L. (2004). Autodesk Revit: implementation in practice. White paper, Autodesk.
452 [7] PROfessional Structural Analysis Program. <https://www.2si.it/it/>
453 [8] Balsamo A, Nardone F, Iovinella I, Ceroni F, Pecce M. Flexural strengthening of concrete beams with
454 EB-FRP, SRP and SRCM: experimental investigation. *Composites B* 2013;46:91–101.
455 [9] Rosenboom O, Rizkalla S. Modeling of IC debonding of FRP-strengthened concrete flexural
456 members. *J Compos Constr* 2008;12(2):168–79.
457 [10] Aiello MA, Leone M, Ombres L. Structural analysis of reinforced concrete beams
458 strengthened with externally bonded FRP (fiber reinforced polymers) sheets. In: Proceedings of the
459 third international conference on “composites in constructions”, Lyon, France, 11–13 July, 2005. p.
460 11–8.
461 [11] Ombres L. Flexural analysis of reinforced concrete beams strengthened with a cement based
462 high strength composite material. *Composite Structures* 2011, 94, 143-155.
463 [12] A.F. Ashour, S.A. El-Refaie and S.W. Garrity. Flexural strengthening of RC continuous beams
464 using CFRP laminates. *Cement and Concrete Composites* 26, 2004, 765–775.
465 [13] Alabdulhady, M. Y., Sneed, L. H. and Carloni C. Torsional behavior of RC beams
466 strengthened with PBO-FRCM composite—an experimental study. *Engineering Structures*, 2017, 136,
467 393-405.
468 [14] Ombres, L. and Verre, S. (2020). Experimental and numerical investigation on the steel
469 reinforced grout (srg) composite-to-concrete bond. *Journal of Composites Science*, 4(4)
470 doi:10.3390/jcs4040182.
471 [15] Bencardino, F., Nisticò, M. and Verre, S. (2020). Experimental investigation and numerical
472 analysis of bond behavior in SRG-strengthened masonry prisms using UHTSS and stainless-steel
473 fibers. *Fibers*, 8(2) doi:10.3390/fib8020008.
474 [16] Ombres, L. and Verre, S. (2019). Numerical modeling approaches of FRCMs/SRG confined
475 masonry columns. *Frontiers in Built Environment*, 5 doi:10.3389/fbuil.2019.00143.
476 [17] Ombres, L. and Verre, S. (2019). Flexural strengthening of RC beams with steel-reinforced
477 grout: Experimental and numerical investigation. *Journal of Composites for Construction*, 23(5)
478 doi:10.1061/(ASCE)CC.1943-5614.0000960.
479 [18] Verre, S. (2019). Three-dimensional numerical modeling of RC beam strengthened in shear
480 with steel reinforced grout (SRG). Paper presented at the Proceedings of the 1st Fib Italy YMG
481 Symposium on Concrete and Concrete Structures, FIBPRO 2019, 64-71.
482 [19] Ombres, L. and Verre, S. (2019). Numerical analysis of the structural response of masonry
483 columns confined with SRG (steel reinforced grout). Paper presented at the IMEKO International
484 Conference on Metrology for Archaeology and Cultural Heritage, MetroArchaeo 2017, 718-722.

- 485 [20] Verre, S., Cascardi, A., Aiello, M. A. and Ombres, L. (2019). Numerical modelling of FRCMs
486 confined masonry column doi:10.4028/www.scientific.net/KEM.817.9.
- 487 [21] Ombres, L. and Verre, S. (2018). Masonry columns strengthened with steel fabric reinforced
488 cementitious matrix (S-FRCM) jackets: Experimental and numerical analysis. Measurement: Journal
489 of the International Measurement Confederation, 127, 238-245.
490 doi:10.1016/j.measurement.2018.05.114.
- 491 [22] Thorenfeldt, E., Tomaszewicz, A., and Jensen, J. J., Mechanical properties of highstrength
492 concrete and applications in design, In Proc. Symp. Utilization of High-Strength Concrete (Stavanger,
493 Norway) (Trondheim, 1987), Tapir.
- 494 [23] Hordijk, D. A. Local Approach to Fatigue of Concrete. PhD thesis, Delft University of
495 Technology, 1991.

496 **Acknowledgement**

497 The authors would like to sincerely thank the owners of the building for having guaranteed access and the
498 possibility to investigate and study the structure.

499 **Conflict of interest statement**

500 The authors declare to have not conflict of interest.